

Mechanism for linear and nonlinear optical effects in monoclinic bismuth borate (BiB_3O_6) crystal

Zheshuai Lin

Fujian Institute of Research on the Structure of Matter, Chinese Academy of Sciences, P.O. Box 143, Fuzhou, Fujian 350002, China and Beijing Center of Crystal Research and Development, Technical Institute of Physics and Chemistry, Chinese Academy of Sciences, P.O. Box 2711, Beijing 100080, China

Zhizhong Wang and Chuangtian Chen^{a)}

Beijing Center of Crystal Research and Development, Technical Institute of Physics and Chemistry, Chinese Academy of Science, P.O. Box 2711, Beijing 100080, China

Ming-Hsie Lee

Department of Physics, Tamkang University, Tamsui, Taipei 251, Taiwan

(Received 20 June 2001; accepted for publication 27 August 2001)

Electronic structure calculations of BiB_3O_6 crystal from first principles are performed based on a plane-wave pseudopotential method. The linear refractive indices and the static second-harmonic generation (SHG) coefficients are also calculated by the SHG formula improved by our group. The calculated values are in good agreement with the experimental values. A real-space atom-cutting method is adopted to analyze the respective contributions of the cation and anionic groups to the optical response. The results show that the contribution of the $(\text{BiO}_4)^{5-}$ anionic group to the SHG coefficients is more pronounced than that of the $(\text{BO}_3)^{3-}$ and $(\text{BO}_4)^{5-}$ groups. © 2001 American Institute of Physics. [DOI: 10.1063/1.1413711]

I. INTRODUCTION

The existence of bismuth triborate, $\text{Bi}_2\text{O}_3\text{O}_6$ (BIBO) was described in early 1962 by Levin and McDaniel in the course of their investigation of the binary phase diagram of $\text{Bi}_2\text{O}_3\text{--B}_2\text{O}_3$.¹ In 1982, the single crystal of BIBO was grown and described by Liebertz^{2,3} and the crystal structure was solved by Frohlich, Bohaty, and Liebertz in 1984.⁴ BIBO crystallizes in the noncentrosymmetric monoclinic space group C2 with cell parameters $a=7.116 \text{ \AA}$, $b=4.993 \text{ \AA}$, $c=6.508 \text{ \AA}$, $\beta=105.6^\circ$ and $Z=2$. The crystal structure consists of $(\text{B}_3\text{O}_6)^{3-}$ rings which form sheets of corner-sharing $(\text{BO}_3)^{3-}$ triangles and $(\text{BO}_4)^{5-}$ tetrahedra in the ratio of 1:2 linked by six-coordinated bismuth cations.⁴

Recent investigations in several laboratories on the linear and nonlinear optical (NLO) properties of BIBO indicate that this crystal is a promising material for effective frequency conversion with $d_{\text{eff}}^{\text{SHG}}=3.2 \text{ pm/V}$,^{5,6} which is higher than that for most other materials currently used, like KTiPO_4 (KTP), $\beta\text{-BaB}_2\text{O}_4$ (BBO), LiB_3O_5 (LBO), or LiIO_3 . Very recently, Becker's group in Koln University (Germany) have grown BIBO crystal of high optical quality with dimensions of $20 \times 20 \times 30 \text{ mm}^3$,⁷ and Teng *et al.* in Shandong University (China) have also grown a crystal of $44.3 \times 23.7 \times 10 \text{ mm}^3$ size using a top-seed solution growth (TSSG) technique.⁸

The origin of these exceptionally large NLO effects in BIBO crystal is still an open problem. So far, a tentative viewpoint on the origin of the large NLO effect of BIBO is that there exist large structure distortion and long-pair electrons in the crystal.^{4,5} In another paper Hellwig, Liebertz, and

Boharty indicate that the semiclassical calculations based on summations of molecular values are not very reliable.⁶ Xue and his co-workers have given calculations of the effects of different chemical bonding structures of boron atoms on the second-order nonlinear optical behavior of several borate crystals from the chemical bond viewpoint. Although they gave some useful results, the calculated values of BIBO differ greatly from the experimental data.⁹

In recent years we have reported *ab initio* energy-band calculations of linear and nonlinear optical effects for BBO,¹⁰ LBO, CBO, and CLBO,¹¹ and KBBF, BABO, KABO, and BPO crystals¹² with a satisfactory explanation for the mechanism of NLO effects. In this article, we will use the *ab initio* energy-band method to calculate the electronic structures of BIBO crystal, and give an explanation for the origin of its NLO effect. In Sec. II, we will briefly introduce the calculation method using the CASTEP package.¹³ In Sec. III, the calculated results and discussion are given.

II. METHOD AND COMPUTATIONAL DETAILS

CASTEP,¹³ a plane-wave pseudopotential total energy package, is used for solving the electronic and band structures as well as linear and nonlinear optical properties of BIBO crystal. The theoretical basis of CASTEP is the density functional theory¹⁴ in the local density approximation (LDA) (Ref. 15) or gradient-corrected LDA developed by Perdew and Wang.¹⁶ Within such a framework, the preconditioned conjugated gradient (CG) band-by-band method¹⁷ used in CASTEP ensures a robust and efficient search of the energy minimum of the electronic structure ground state. The optimized pseudopotential^{18–20} in the Kleinman–Bylander

^{a)}Electronic mail: cct@cl.cryo.ac.cn

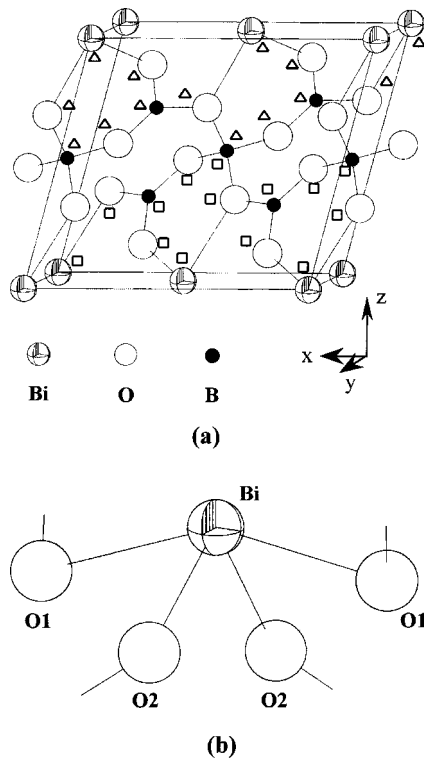


FIG. 1. (a) Structure of the unit cell in the BIBO crystal. (b) Structure of the BiO_4 group in the BIBO crystal.

form²¹ for Bi, B, and O allows us to use small plane-wave basis sets without compromising the accuracy required by our study.

It is well known that the band-gap calculated by the LDA is usually smaller than the experimental data. A scissors operator^{22,23} is also used to shift upward all the conduction bands in order to agree with measured values of the band gap.

Our group and co-workers have reviewed the calculation methods for second-harmonic generation (SHG) coefficients.¹⁰ The static limit of the SHG coefficients plays the most important role in the application of SHG crystals, so we adopt the formula presented by Rashkeev, Lambrecht, and Segall,²⁴ and improved by us,¹⁰

$$\chi^{\alpha\beta\gamma} = \chi^{\alpha\beta\gamma}(\text{VE}) + \chi^{\alpha\beta\gamma}(\text{VH}) + \chi^{\alpha\beta\gamma}(\text{two bands}),$$

where $\chi^{\alpha\beta\gamma}(\text{VE})$ and $\chi^{\alpha\beta\gamma}(\text{VH})$ give the contributions to $\chi_i^{(2)}$ from virtual-electron processes and virtual-hole processes, respectively; $\chi^{\alpha\beta\gamma}(\text{two bands})$ is the contribution to $\chi_i^{(2)}$ from the two-band processes. The formulas for calculating $\chi^{\alpha\beta\gamma}(\text{VE})$, $\chi^{\alpha\beta\gamma}(\text{VH})$, and $\chi^{\alpha\beta\gamma}(\text{two bands})$ are given in Ref. 10.

The geometric parameters of BIBO crystal are given above,⁴ and the basic structural features are shown in Fig. 1(a). There are two $(\text{BiO}_4)^{5-}$ [Fig. 1(b)], two $(\text{BO}_4)^{5-}$, and four $(\text{BO}_3)^{3-}$ groups in a unit cell, respectively. The prominent structure feature is that the borate triangles which should be dominant in their effect according to the anionic group theory are highly distorted. The location of the boron atom with 0.044 Å out of the oxygen plane is one of the farthest found in borate complexes, and the angles of the

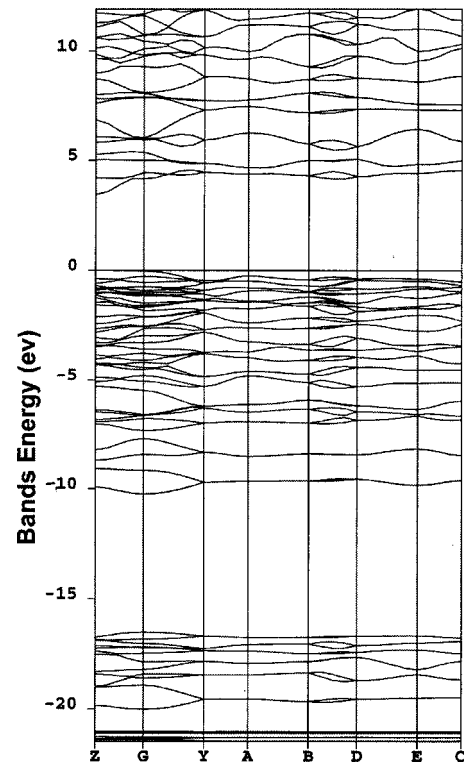


FIG. 2. Band structure of BIBO.

O–B–O bonds are found to be 128.8°, 121.2°, and 110.3°. Furthermore, the bismuth ion carries a lone-pair electron oriented parallel to the twofold axis. All these structural factors should have their specific influence on the electronic and band structures of BIBO and, consequently, on the optical properties. An *ab initio* pseudopotential calculation can re-

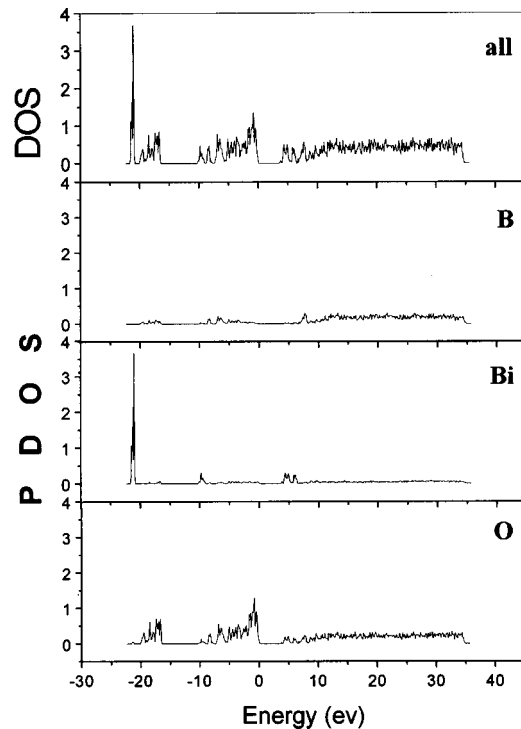
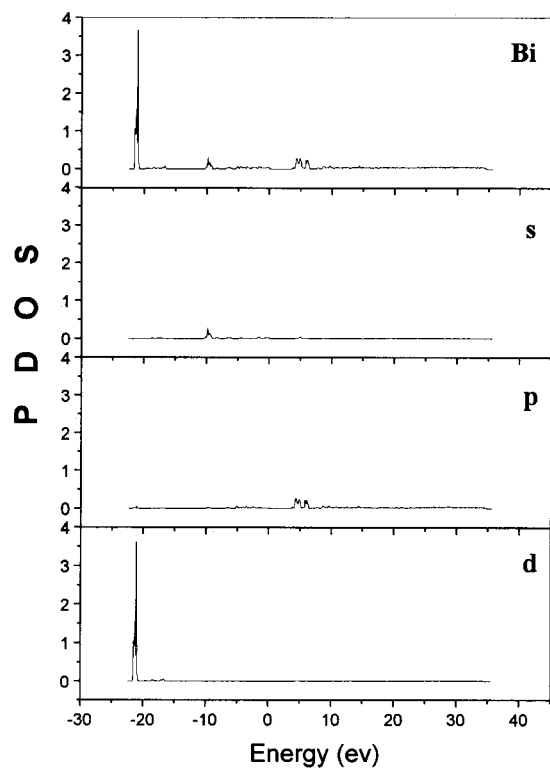
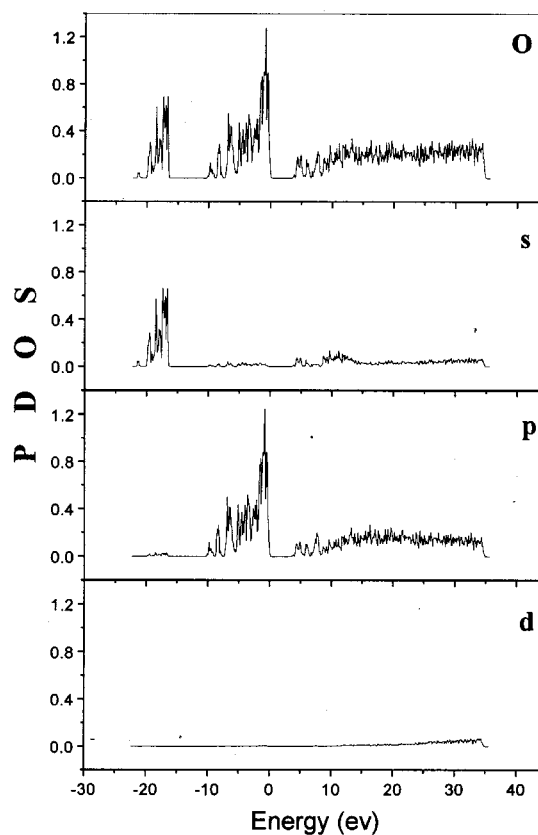


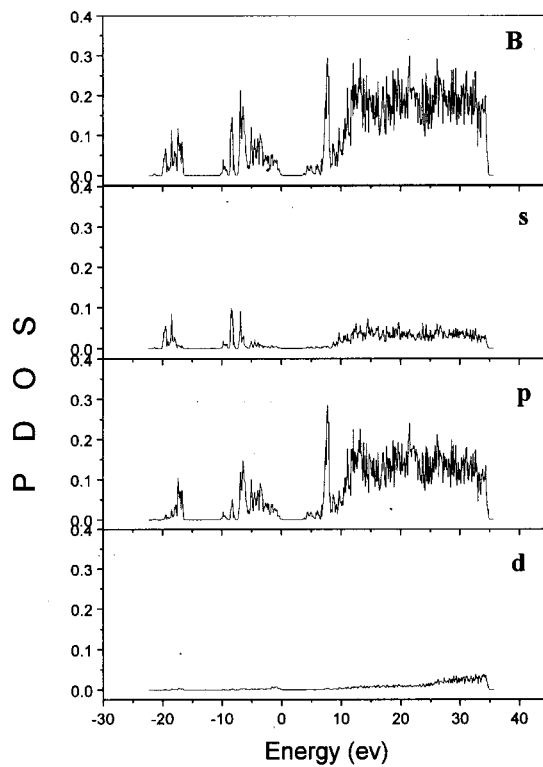
FIG. 3. DOS and partial DOS plot of the BIBO crystal.



(a)



(b)



(c)

FIG. 4. Orbital-resolved PDOS of (a) Bi, (b) O, and (c) B in BIBO.

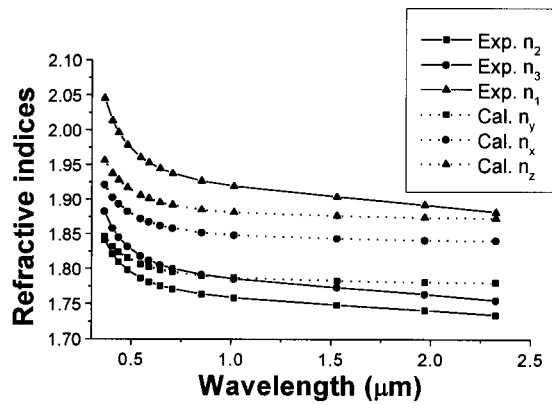


FIG. 5. Calculated and experimental dispersion curve of refractive indices of BIBO.

veal the effects in a straightforward manner. With a real-space atom-cutting method, the respective actions of the anionic groups and cations on the optical properties may be recognized and understood. This is the goal of the present article.

III. RESULTS AND DISCUSSION

A. Energy-band structure

The computed energy-band structure and the total density of states (DOS) and partial density of states (PDOS) of BIBO crystal are shown in Figs. 2 and 3, respectively. A directed band gap of 3.45 eV at the Z point computed is obtained, which is smaller than the experimental value of 4.32 eV (~ 286 nm).⁵ Both the band structure and DOS figures show many small minigaps among the highly located bands. This is typical of the electronic structure of a molecular crystal. All energy bands become flat along high-symmetry lines in the Brillouin zone (BZ). Maybe this is the reason for every NLO coefficient of BIBO being relatively large. Figure 4 shows the orbital-resolved PDOS of the various atoms. It can be seen that the energy bands are divided into three regions. The lower region is located below -15 eV and mainly consists of $2s$ orbitals of oxygen atoms, but in Fig. 4(a) it is shown that there exists a relatively high peak at about -21 eV, which comes from the inner $5d$ components of the Bi atom. The middle region is the valence band (VB) from about -10 to 0 eV. The valence bands are mainly com-

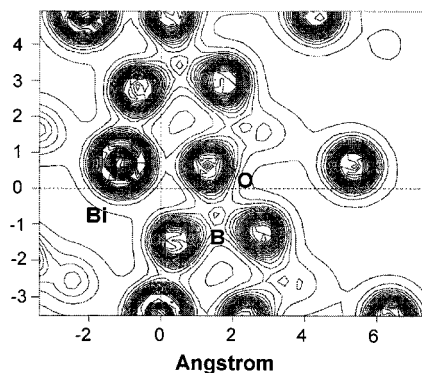


FIG. 6. Charge density of the plane shown in Fig. 1.

TABLE I. Refractive indices of BIBO in the static limit derived from only $(\text{BO}_3)^{3-}$, $(\text{BO}_4)^{5-}$, or $(\text{BiO}_4)^{5-}$ wave functions.

	$n_2(n_y)$	$n_3(n_x)$	$n_1(n_z)$	Δn
Total	1.7792	1.8391	1.8717	0.0925
Only BO_3	1.5242	1.5514	1.5991	0.0749
Only BO_4	1.3782	1.4014	1.4240	0.0458
Only BiO_4	1.6388	1.6922	1.6746	0.0534

posed of $2p$ orbitals of oxygen atoms in various oxygen-containing groups like $(\text{BO}_3)^{3-}$, $(\text{BO}_4)^{5-}$, and $(\text{BiO}_4)^{5-}$. The atom-resolved PDOS figure shows that a small fraction of the orbitals of B and Bi atoms are also mixed in the valence bands. The upper one is the conduction band (CB), with a total width of about 5 eV. Figures 3 and 4 indicate that the CB is mainly composed of the $2p$ valence orbitals of oxygen and boron atoms, but some $6p$ orbitals of the bismuth atom are also present at the bottom and almost determine the band gap of the crystal. This could be a major reason why BIBO has a narrower band gap compared with other borate NLO crystals.

B. Linear optical susceptibility

It is well known that the refractive indices are obtained theoretically from the imaginary part of the dielectric function through the Kramer–Kronig transformation. The imaginary part can be calculated with the matrix elements that describe the electronic transition between the ground and excited states in the crystal considered. The calculation formulas are given in Ref. 10. For BIBO, the calculated and experimental values of the refractive indices are plotted in Fig. 5. It can be seen that the calculated results are in good agreement with experimental values.

To investigate the influence of the ions on the optical response of BIBO, the real-space atom-cutting method has been used. In a previous paper, it was found that the charge density around the cation (M) is spherical.¹⁰ Figure 6 shows the calculated charge distribution which also indicates that there is a sphere-like distribution around the Bi^{3+} ion with an apparent electron density overlap between bismuth or boron and oxygen atoms. This fact shows that the Bi appears as a weak ion and is not an isolated cation in bismuth borate, which is very different from alkali and earth-alkali metal borates. Thus, we cannot cut out the cation Bi^{3+} , but should choose $(\text{BiO}_4)^{5-}$ as a whole to analyze its contribution to optical responses. We choose the cutting radius of Bi to be 1.50 Å, which is approximately equal to its covalent radius. Following the rule of keeping the cutting spheres of M and O in contact, the cutting radius of O is set to be 1.10 Å. It must be pointed out that the definition of the boundary of two nearest ions is given by the point at which the charge density in real space reaches a local minimum. For the boron atom the covalent radius (0.88 Å) is also chosen as its cutting radius.

Our conclusions from the above calculations are the following: (i) The calculated refractive indices (Fig. 5) are in good agreement with experimental values. This agreement proves the validity of our investigation of BIBO with the

TABLE II. Calculated and experimental values of the SHG coefficients of BIBO and analysis using the real-space atom-cutting method (in pm/V).

	d_{22}	d_{16}	d_{14}	d_{23}
Experimental ^a	± 2.53	± 2.8 ± 2.3	± 2.4 (d_{123}) ± 2.4 (d_{312}) ± 2.3 (d_{231})	∓ 1.3 (d_{233}) ∓ 0.9 (d_{332})
Calculated	-2.95	-2.55	-1.16	-1.17
Only_BO ₃	-0.233	-0.628	0.372	0.243
Only_BO ₄	-0.118	-0.334	0.391	0.050
Only_BiO ₄	-2.829	-2.090	-1.412	-1.182
Sum	-3.180	-3.052	-0.649	-0.889

^aReferences 5 and 6.

density functional theory. (ii) Table I also shows that for BIBO the contributions of various anionic groups such as $(\text{BO}_3)^{3-}$, $(\text{BO}_4)^{5-}$, and $(\text{BiO}_4)^{5-}$ groups to the refractive indices are comparable with each other, but the contribution of the $(\text{BO}_3)^{3-}$ group to anisotropy seems rather important.

C. SHG coefficients

According to the computational formula given in Ref. 10, the SHG coefficients of BIBO crystal have been calculated from the band wave functions and band energies. The theoretical and experimental SHG values are listed in Table II. In order to calculate the respective contributions of the anionic groups to the SHG coefficients, we adopt the real-space atom-cutting method. This method means that if the contribution of ion A to the n th-order polarizability is denoted as $\chi^{(n)}(A)$, we can obtain it by cutting all ions except A from the original wave functions $\chi^{(n)}(A) = \chi^{(n)}$ (all ions except A are cut). We have used the same cutting radius as mentioned in Sec. II B in the calculations of SHG coefficients. The decomposition results are also given in Table II.

These calculated results lead to the following conclusions: (1) Our plane pseudopotential approach is suitable for studying the SHG coefficients of BIBO crystal at zero-frequency approximation. We can see that the agreement between calculated and experimental values of the SHG coefficients is very good. For the greater d_{22} and d_{16} coefficients the contributions from the anionic group $(\text{BiO}_4)^{5-}$ exceed 90%. For the smaller d_{14} and d_{23} coefficients the contributions of $(\text{BiO}_4)^{5-}$ exceed 100% of their calculated values, but at the same time the contributions from $(\text{BO}_3)^{3-}$ and $(\text{BO}_4)^{5-}$ are opposite in sign. Compared with the contribution from $(\text{BiO}_4)^{5-}$, these from the other anionic groups $(\text{BO}_3)^{3-}$ and $(\text{BO}_4)^{5-}$ are not important, but that of the $(\text{BO}_3)^{3-}$ anionic group is slightly greater than that of $(\text{BO}_4)^{5-}$. These calculated results clearly indicate that the exceptionally large d_{ij} coefficients of BIBO crystal mainly come from the contribution of the BiO_4 group.

In previous studies we found that in the borate crystals the nonlinear optical effects mainly come from the $(\text{BO}_3)^{3-}$ and $(\text{BO}_4)^{5-}$ anionic groups.¹⁰⁻¹² However, as indicated in the above-mentioned discussions for BIBO crystal, its NLO effects mainly originate from $(\text{BiO}_4)^{5-}$. Why is this so? From its structure we find that the $(\text{BO}_3)^{3-}$ triangles are heavily distorted (the B atom is located far from the oxygen atom plane) and the B_3O_6 rings are also far from a plane, so

TABLE III. Comparison of the experimental and calculated SHG coefficients of BIBO from this work and Xue *et al.* (units: pm/V).

	Experimental ^a	This work	Xue <i>et al.</i> ^b
d_{22}	± 2.53	-2.95	0.30
d_{16}	± 2.8 ± 2.3	-2.55	2.49
d_{14}	± 2.4 (d_{123}) ± 2.4 (d_{312}) ± 2.3 (d_{231})	-1.16	0.18
d_{23}	∓ 1.3 (d_{233}) ∓ 0.9 (d_{332})	-1.17	-2.82

^aReferences 5 and 6.^bReference 9.

the BO_3 group cannot contribute much to the NLO effects. Usually, the bismuth ion is regarded as being six-coordinated. However, the two Bi-O bonds in the BiO_6 group of the crystal, for example $r_{\text{Bi-O}(3)} = 2.629 \text{ \AA}$, are too long to be accepted as a chemical bond. Obviously, the Bi-O(3) bonds are very weak. The two O(3) atoms are included in another BiO_4 group cut out, so their contributions to both linear and nonlinear optical responses are already accounted for. These structural factors lead us to choose the $(\text{BiO}_4)^{5-}$ group as a NLO active group to calculate its contributions to the SHG effects. On the other hand, because the $(\text{BiO}_4)^{5-}$ group is a distorted tetragonal [see Fig. 1(b)] and, meanwhile, has a lone-pair electron of Bi in this $(\text{BiO}_4)^{5-}$ type, it should have a greater contribution to the SHG effects. The calculated results confirm this point of view (see Table II). Moreover, we chose the Bi^{3+} cation as a NLO unit to calculate its contributions to the SHG effects. The results show that the contribution of the Bi^{3+} cation to the SHG coefficients is much less than that of the $(\text{BiO}_4)^{5-}$ group (for example, $d_{22}^{\text{only Bi}} = -0.64 \text{ pm/V}$, $d_{16}^{\text{only Bi}} = -0.66 \text{ pm/V}$, $d_{14}^{\text{only Bi}} = -0.34 \text{ pm/V}$, and $d_{16}^{\text{only Bi}} = -0.34 \text{ pm/V}$). This implies that the electronic transfer between Bi and O in the $(\text{BiO}_4)^{5-}$ group is the main reason for producing relative larger SHG coefficients for BIBO crystal. Because the semi-empirical calculations based on the chemical bonding cannot account for all electronic effects on the NLO effects,⁹ the calculated results differ greatly from the experimental ones. In Table III we list our and Xue's calculated values⁹ for comparison.

Finally, we have also calculated the contributions of the anionic groups $(\text{BO}_3)^{3-}$, $(\text{BO}_4)^{5-}$, and $(\text{BiO}_4)^{5-}$ in the crystal environment to the SHG effects by means of the GAUSSIAN'92 program²⁵ and our own SHG calculation program. The results show that the contributions of the $(\text{BiO}_4)^{5-}$ group are about ten times greater than those of the $(\text{BO}_3)^{3-}$ or $(\text{BO}_4)^{5-}$ groups. The qualitative conclusion is the same as that of the present *ab initio* energy-band calculation.

IV. CONCLUSION

The linear and nonlinear optical coefficients of BIBO crystal have been calculated from first principles by means of a plane-wave pseudopotential method. The calculated results are in good agreement with experimental values. The respec-

tive contributions from $(\text{BO}_3)^{3-}$, $(\text{BO}_4)^{5-}$, and $(\text{BiO}_4)^{5-}$ groups are analyzed by use of a real-atom cutting method. As a result, the origin of the large NLO effect of BIBO crystal is well revealed. The contribution from the $(\text{BiO}_4)^{5-}$ group is predominant (giving almost 90% of the total value), and it originates from completely electronic effects, including those from lone-pair electrons.

ACKNOWLEDGMENTS

This work was supported by the Chinese National Key Basic Research Project. Support in computing facilities from the Computer Network Information Center is gratefully acknowledged. M.H.L. acknowledges funding support from NSC 89-2112-M-032-026.

- ¹E. M. Levin and C. L. McDaniel, *J. Am. Ceram. Soc.* **45**, 355 (1962).
- ²J. Liebertz, *Z. Kristallogr.* **158**, 319 (1982).
- ³J. Liebertz, *Prog. Cryst. Growth Charact.* **6**, 361 (1983).
- ⁴R. Frohlich, L. Bohaty, and J. Liebertz, *Acta Crystallogr., Sect. C: Cryst. Struct. Commun.* **40**, 343 (1984).
- ⁵H. Hellwig, L. Liebertz, and L. Bohaty, *J. Appl. Phys.* **88**, 240 (2000).
- ⁶H. Hellwig, L. Liebertz, and L. Bohaty, *Solid State Commun.* **109**, 249 (1999).
- ⁷P. Becker, J. Liebertz, and L. Bohaty, *J. Cryst. Growth* **203**, 149 (1999).
- ⁸B. Teng, J. Y. Wang, Z. P. Wang, H. Liu, X. B. Hu, R. G. Liu, J. Q. Wei, and Z. S. Shao, *Chin. Sci. Bull.* **46**, 987 (2001).
- ⁹D. Xue, K. Betzler, H. Hesse, and D. Lammers, *Solid State Commun.* **114**, 21 (2000).
- ¹⁰J. Lin, M. H. Lee, Z. P. Liu, C. T. Chen, and C. J. Pickard, *Phys. Rev. B* **60**, 13380 (1999).
- ¹¹Z. S. Lin, J. Lin, Z. Z. Wang, C. T. Chen, and M. H. Lee, *Phys. Rev. B* **62**, 1757 (2000).
- ¹²Z. S. Lin, Z. Z. Wang, C. T. Chen, S. K. Chen, and M. H. Lee (unpublished).
- ¹³CASTEP 3.5 program, Molecular Simulation Inc. (1997).
- ¹⁴R. G. Parr and W. T. Yang, *Density Functional Theory of Atom-Molecules* (Oxford University Press, Oxford, 1989).
- ¹⁵W. Kohn and L. J. Sham, *Phys. Rev.* **140**, 1133 (1965).
- ¹⁶P. Perdew and Y. Wang, *Phys. Rev. B* **45**, 13244 (1992).
- ¹⁷M. C. Payne, M. P. Teter, D. C. Allan, T. A. Arias, and J. O. Joannopoulos, *Rev. Mod. Phys.* **64**, 1045 (1992).
- ¹⁸A. M. Rappe, K. M. Rabe, E. Kaxiras, and J. D. Joannopoulos, *Phys. Rev. B* **41**, 1227 (1990).
- ¹⁹J. S. Lin, A. Qtseish, M. C. Payne, and V. Heine, *Phys. Rev. B* **47**, 4174 (1993).
- ²⁰M-H. Lee, J-S. Lin, M. C. Payne, V. Heine, V. Milman, and S. Crampin (unpublished).
- ²¹L. Kleinman and D. M. Bylander, *Phys. Rev. Lett.* **48**, 1425 (1982).
- ²²R. W. Godby, M. Schluter, and L. J. Sham, *Phys. Rev. B* **37**, 10159 (1988).
- ²³C. S. Wang and B. M. Klein, *Phys. Rev. B* **24**, 3417 (1981); M. S. Hybertsen and S. G. Louie, *ibid.* **34**, 5390 (1988).
- ²⁴S. N. Rashkeev, W. R. L. Lambrecht, and B. Segall, *Phys. Rev. B* **57**, 3905 (1998).
- ²⁵*Gaussian'92, Revision A* (Gaussian, Pittsburgh, PA, 1992).